Hindawi
Adsorption Science & Technology
Volume 2022, Article ID 1019746, 15 pages
https://doi.org/10.1155/2022/1019746

Review Article

Adsorption Properties of NF_3 and N_2O on Al- and Ga-Doped Graphene Surface: A Density Functional Theory Study

Qilin Yi, Gang Wei, Zhengqin Cao, Xiaoyu Wu, and Yuanyuan Gao

College of Electrical Engineering, Chongqing University of Science and Technology, Chongqing 401331, China

Correspondence should be addressed to Gang Wei; eecqweig@163.com

Received 15 August 2022; Revised 9 October 2022; Accepted 18 October 2022; Published 15 November 2022

Academic Editor: Muhammad Raziq Rahimi Kooh

SF_6/N_2 gas mixture decomposition components can reflect the operation status inside GIS, and be used for fault diagnosis and monitoring inside GIS. NF_3 and N_2O are the characteristic decomposition components of SF_6/N_2 mixed gas. In order to find a potential gas sensitivity material for the detection of NF_3 and N_2O. This paper investigated the adsorption properties of NF_3 and N_2O on Al- and Ga- doped graphene monolayers based on density functional theory. Through the analysis of adsorption distance, charge transfer, adsorption energy, energy band structure, etc., the results indicated that the adsorption effect of Al- and Ga-doped graphene to NF_3 and N_2O are probably good, and these nanomaterials are potential to apply for the monitoring of GIS internal faults.

1. Introduction

SF_6 has been extensively adopted for high-voltage gas insulation devices due to its superb arc extinguishing and insulation abilities. However, it has a strong greenhouse effect [1–3]. Concurrently, the addition of N_2 can greatly reduce the use of SF_6 gas without significantly affecting the insulation performance, which is of great importance in achieving energy conservation and emission reduction [4–7]. However, SF_6/N_2 mixed gas under partial discharge (PD) or partial overheating conditions will produce gases such as NF_3, SO_2, CO_2, and N_2O [8]. It is a feasible technical method to comprehend the fault diagnosis of SF_6/N_2 mixed gas insulation equipment by monitoring this characteristic component decomposition information.

As the research hotspot of gas sensing materials in the sensor field, graphene has become an irreplaceable material with its ultrahigh electron mobility and specific surface area (SSA), along with superb mechanical characteristics [9–12]. Compared to other sensing materials, the following documents are available. According to He et al. C_2H_2 gas was analyzed for its sensing properties as well as electronic characteristics on diverse boron nitride nanotubes-modified transition metal oxide (Fe_2O_3, TiO_2, and NiO) nanoparticles [13]. It was found that the conductivity of C_2H_2 gas on the three transition metal oxides and modified boron nitride nanotubes was different, especially on Fe_2O_3 and TiO_2. In his studies of the gas sensing properties of single-walled carbon nanotubes doped with gold atoms for SO_2 and H_2S. Chen et al. found that SO_2 and H_2S have good adsorption properties on gold doped single-walled carbon nanotubes [14]. Syaahiran et al. implemented the DFT method to analyze CO, H_2S, and H_2 for their gas sensing performances on (WO_3) n $(n = 2 - 4)$ doped Cr [15]. The results indicate that when compared with undoped clusters (WO_3) n $(n = 2 - 4)$, the energy gap of chromium-doped tungsten oxide clusters decreases $(CrW_{n-1}O_{3n})$ $(n = 2 - 4)$, the reactivity increases and the stability is improved. Syaahiran et al. studied the interaction of CO gas on chromium doped-tungsten oxide/graphene composites [16]. From the energy gap, surface activity, and binding energy, it is found that chromium-doped tungsten oxide/graphene composite has a strong adsorption effect on CO.

Many scholars have studied the gas sensors of atom doped graphene, such as Mn, Pd, and Pt, to better study the interaction between graphene materials and gas molecules and to explore the gas-sensing characteristics of gases onto doped and intrinsic graphene surfaces. Gui et al.

Table 1: Formation energy of Al- and Ga-doped Gra at T, B, H, and R sites.

Configuration	Top(T)	Bridge(B)	Heart(H)	Replacement(R)
$E_{Al-form}$(eV)	-1.058	-0.835	-1.093	-1.253
$E_{Ga-form}$(eV)	-1.236	-1.034	-1.025	-1.076

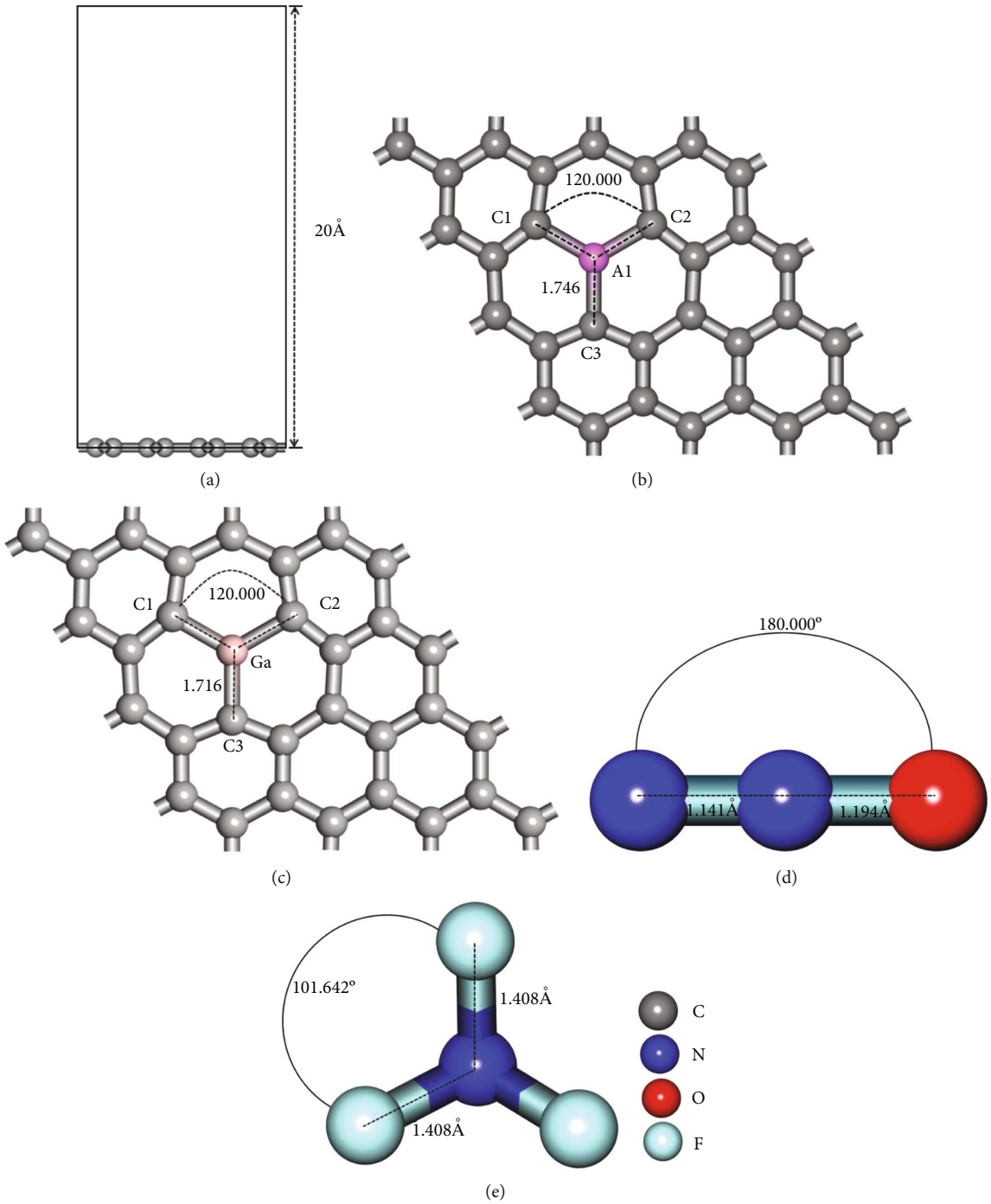

Figure 1: Geometry optimization structure of Al- and Ga-doped graphene, N_2O, and NF_3 ((a) side view of Al-doped graphene; (b) top view of Al-doped graphene; (c) top view of Ga-doped graphene; (d) N_2O; (e) NF_3).

through DFT calculation, studied adsorption properties for typical oil soluble gases (C_2H_2, CH_4, and CO) in transformers by doping Mn atoms at graphene bridge sites [17]. The gas sensing mechanism was analyzed by using the density of states (DOS) and molecular orbital theory. As a result, manganese-doped graphene was the potential gas-sensing

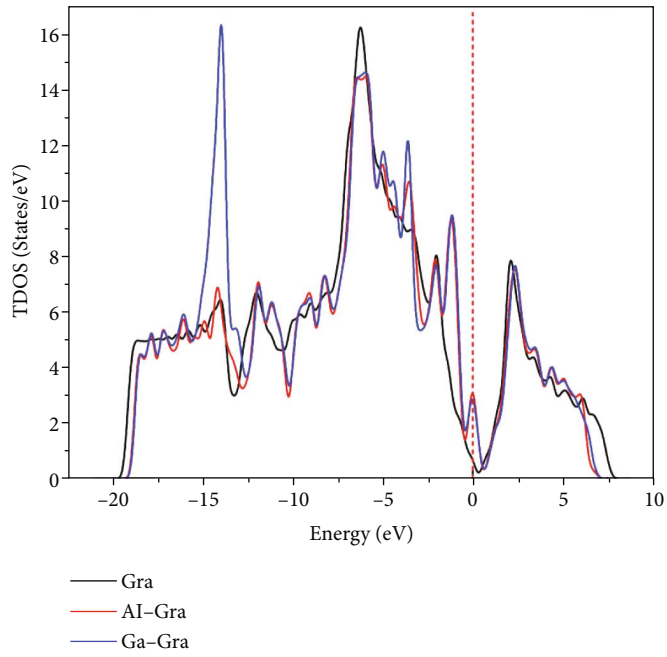

Figure 2: The TDOS configuration of graphene, Al- and Ga-doped Graphene.

substance in the detection of CO and C_2H_2. According to the literature, gas adsorption is more evident due to the doping of transition metals [18]. It is confirmed that doped graphene shows better gas sensing performance than intrinsic graphene, and metal doping remarkably enhances graphene chemical activity and adsorption performance.

According to above-mentioned, this paper studies the gas sensitivity of Al-doped Gra and Ga-doped Gra to NF_3 and N_2O gas molecules based on DFT. This work will guide the manufacturing of gas sensors and provide basic gas sensitivity information, as well as aluminum-doped graphene or gallium-doped graphene as a potential candidate for resistance chemical sensors for GIS internal fault diagnosis.

2. Computational Details

The present work conducted first-principle calculation by Dmol^3 quantum chemistry module from Materials Studio [19–21]. Perdew Burke ernzerho (PBE) function of the generalized gradient approximation (GGA) is used for managing the electron exchange relation [22]. Besides, double numerical plus polarization (DNP) is selected to be the atomic orbital basis group. The maximum atomic displacement, energy convergence accuracy, orbital tailing, and maximum force are set to 5×10^{-3} Å, 1.0×10^{-5} Ha, 0.005Ha, and 0.05 eV/Å, respectively [23, 24]. Also, to ensure precision in calculating total energy, this work established global orbital cut-off radius and self-consistent field error at 4.5 Å and 1.0x10^{-6}Ha, respectively, Additively, a $2\times2\times1$ Brillouin k-point grid space was set [25, 26]. Dispersion force was controlled by using DFT-D (Grimme) approach, and the charge transfer amount (Q_d) in the adsorption process was determined based on the Hirshfield approach [16, 27]. The total charge number $Q_d > 0$, represents the transfer of electrons to the doped graphene surface from gas molecules, and the negative value stands for the opposite electron transfer path. Further, the definition of adsorption energy (E_{ad}) is shown in [28]:

$$E_{ad} = E_{X-\text{Graphene/gas}} - E_{X-\text{Graphene}} - E_{\text{gas}}. \quad (1)$$

$E_{X-\text{Graphene/gas}}$, $E_{X-\text{Graphene}}$, E_{gas} represent energy of gas adsorption on metal doped graphene, the energy of an Al-doped graphene and Ga-doped graphene surface, and Energy of gas, respectively. Generally, $E_{ad} > 0$ means that the adsorption process does not occur automatically, while $E_{ad} < 0$ means that the adsorption process is automatic [29].

3. Results and Discussion

3.1. The Optimization of Al-Doped Graphene, Ga-Graphene, NF_3, and N_2O. Firstly, the adsorption characteristics of the aluminum and gallium atoms onto the graphene surface are discussed through the formation energy (E_{form}). Aluminum and gallium atoms E_{form} moving onto the graphene surface is defined in [30]:

$$E_{\text{form}} = E_{X-\text{Graphene}} - E_X - E_{\text{Graphene}}. \quad (2)$$

$E_{X-\text{Graphene}}$, energy after doping graphene into aluminum and gallium; E_X and E_{Graphene} are the initial energies of aluminum, gallium, and graphene substrates, respectively. We considered the doping configurations of the top, bridge, heart, and replacement sites. By comparing the formation energies of different doping structures in Table 1, we found that the configuration of the replacement site is the most stable.

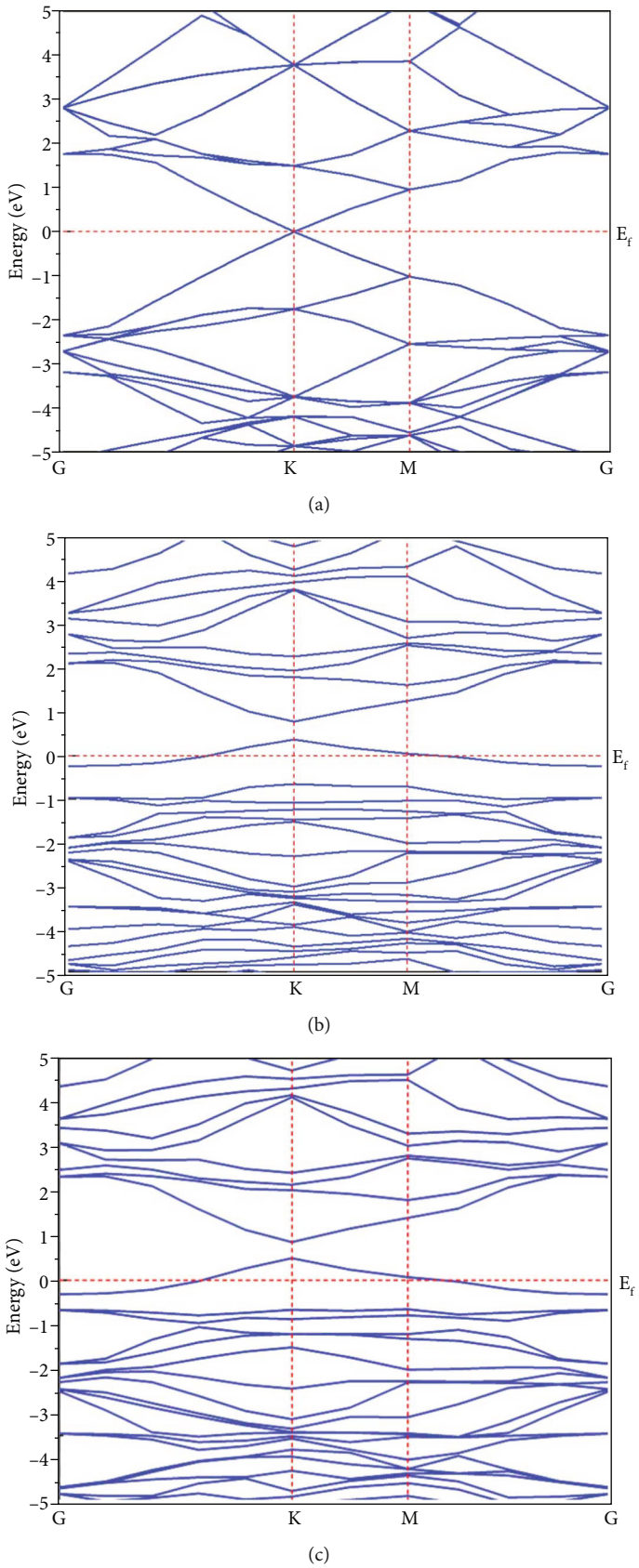

Figure 3: The band structure of undoped graphene, Al- and Ga-Graphene ((a) Undoped Graphene; (b) Al-Graphene; (c) Ga-Graphene).

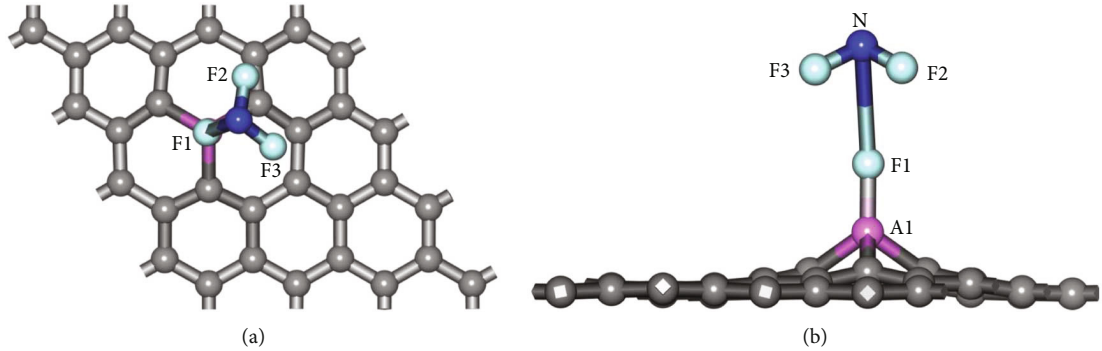

Figure 4: Adsorption configuration of NF_3 adsorbed on Al-Graphene: (a) top view; (b) side view.

Table 2: The E_{ad}, Q_t, and structural parameters of the NF_3 adsorbed on Al-Graohene.

Configuration	E_{ad}(eV)	Q_t(e)	$d_{F1\text{-}Al}$(Å)	$d_{F1\text{-}N}$(Å)	∠F1-N-F2(°)	∠F2-N-F3(°)
F1-Al-Gra	-1.476	0.291	1.689	3.072	75.591	103.457

Figure 1 presents optimal geometry for aluminum-doped graphene, gallium-doped graphene, NF_3, and N_2O, with bond angle and bond length being expressed as ∘and *Å*, respectively. According to Figure 1(a), the aluminum-doped graphene surface is composed of $(4 \times 4 \times 1)$ supercells with a 20 Å(1 Å = 10^{-10} m) vacuum layer for reducing the interaction of neighboring clusters and for preventing interactions between planes resulting from periodic boundary conditions [31]. The optimal top view for aluminum-doped graphene exhibit in Figure 1(b). The bond length between the Al and the surrounding three carbon atoms is 1.746 Å, which is increased by 0.321 Å compared with the carbon-carbon before doping, since aluminum has a larger atomic orbital radius than carbon. The ∠C1-Al-C2 is 120°, which remained unchanged from that before doping. The optimal top view for gallium-doped graphene is shown in Figure 1(c). Optimal N_2O and NF_3 gas molecules structures are shown in Figures 1(d) and 1(e).

Figure 2 shows the TDOS for graphene, Al- and Ga-doped graphene. The structural properties of doped-graphene are further analyzed through TDOS. Contrast undoped graphene, it is known that the charge distribution of TDOS increases remarkably near the Fermi level after doping aluminum and gallium relative to intrinsic graphene, suggesting that aluminum and gallium doping enhances graphene structure conductivity.

The band structure of intrinsic graphene is shown in Figure 3(a). It can be seen from the figure that the valence band and conduction band are almost tangent at the Fermi energy level, and the band gap is 0.005 eV, approaching 0 eV. However, after doping aluminum atoms, as shown in Figure 3(b), the valence band moves up and intersects with the E_f. After doping, the band gap of graphene has obviously increased, which is 0.227 eV. At the same time, a new energy level has been introduced near the E_f, indicating that the electrical and physical properties of graphene have changed significantly due to the doping of aluminum atoms as shown in Figure 3(c). Doped gallium atoms have similar properties. The influence of aluminum-doped graphene and gallium-doped graphene on gas adsorption characteristics needs to be further studied.

3.2. The Adsorption Properties of NF_3 on Aluminum-Doped Graphene. Different original approach sites for NF_3 on aluminum doped sites were calculated for obtaining adsorption structure with the highest stability to further analyze the adsorption characteristics of aluminum-doped graphene on target gas. A characteristic adsorption structure is obtained following optimization. Figure 4 shows its top view and side view. Table 2 displays the charge transfer and adsorption energy, together with structural parameters.

As observed from the adsorption structure in (Figures 4(a) and 4(b)). The bond length formed by A1-F1 is 1.689 Å, and the number of electrons transferred from aluminum-doped graphene surface onto NF_3 reaches 0.291e. Noteworthily, the NF_3 structure alters the following adsorption, among them, the F1-N bond length increases to 3.072 Å, and the angle of F1-N-F2 becomes 75.591°. The E_{ad} of NF_3 onto aluminum-doped graphene surface reaches -1.476 eV. From the perspective of electron transfer and E_g, the reaction of NF_3 gas is strongest when F atom is close to the aluminum-doped graphene surface.

Figure 5(a) shows the TDOS for NF_3 on aluminum-doped graphene surface. The TDOS showed significant changes at -14 eV, -9.2 eV, -7.3 eV, -5.4 eV, -3.4 eV, and other positions when compared with the nonadsorbed gas. Due to the outermost electrons of atoms contributing the most during adsorption, just PDOS for Al-3p, F-2p, and N-2p is discussed. From the PDOS in Figure 5(b), we can see that for the above orbitals, their overlapped peaks can be seen at approximately, -9.3 eV, -7.3 eV, -3.9 eV, Fermi level, and 5.2 eV. PDOS and TDOS analyses implicit that there are great interaction between NF_3 and aluminum-doped graphene.

Figure 6 displays the difference in electron density of NF_3 adsorbed onto aluminum-doped graphene surfaces

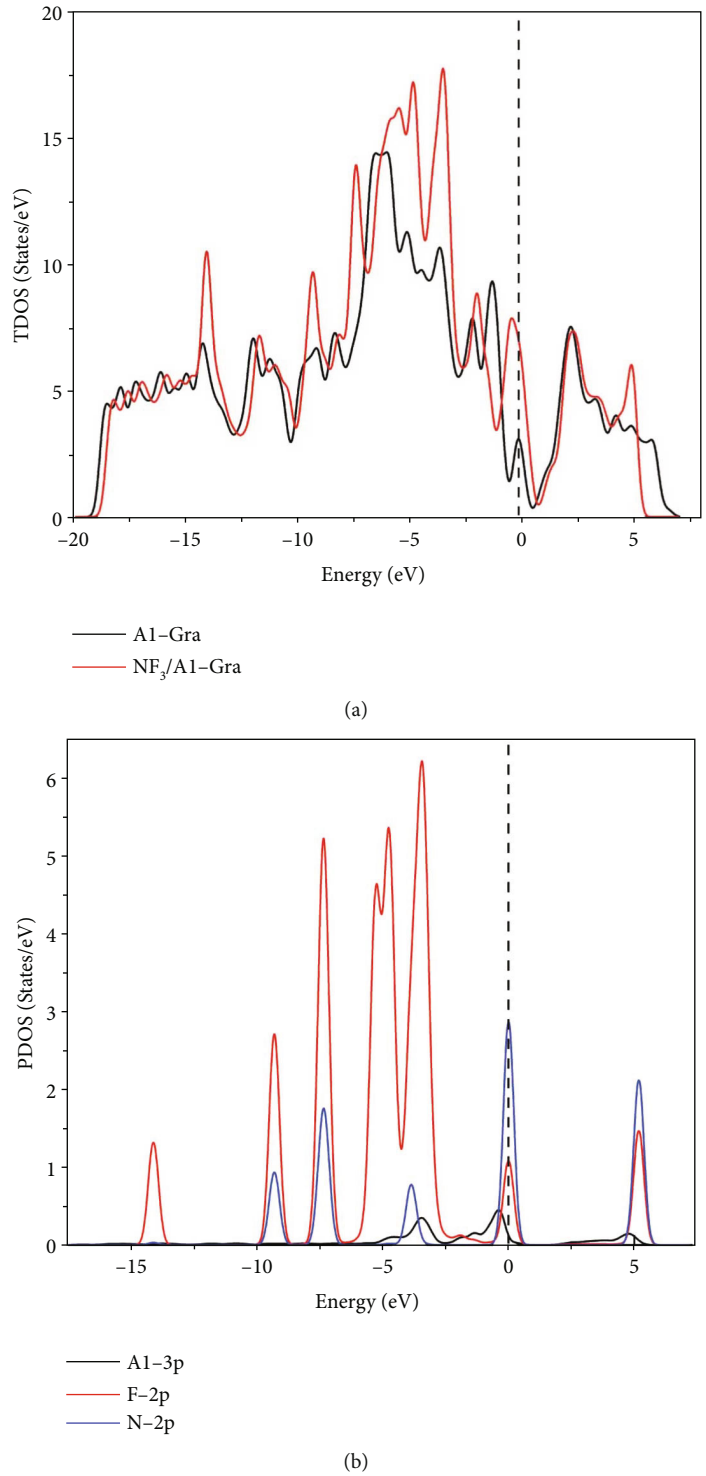

Figure 5: TDOS before and after NF_3 adsorption and PDOS of the main interacting atoms ((a) TDOS; (b) PDOS).

from different sides, in which the red and blue areas indicate elevated and declined electron density, respectively. The post-gas adsorption charge distribution is analyzed intuitively based on the difference in electron density. From Figure 6, it shows that the red area around the F atom shows that electrons are received, while the blue area around the N atom, Al atom, and C atom indicates that electrons are lost due to the reduction in electron density. Gas molecules are suggested to play the role of electron acceptors, while Al-Graphene is the electron donors. Therefore, NF_3 molecules bring drastic changes in electron density to the surface of aluminum-doped graphene.

Collectively, based on the structural parameters of DOS, adsorption energy, and charge transfer, together with the

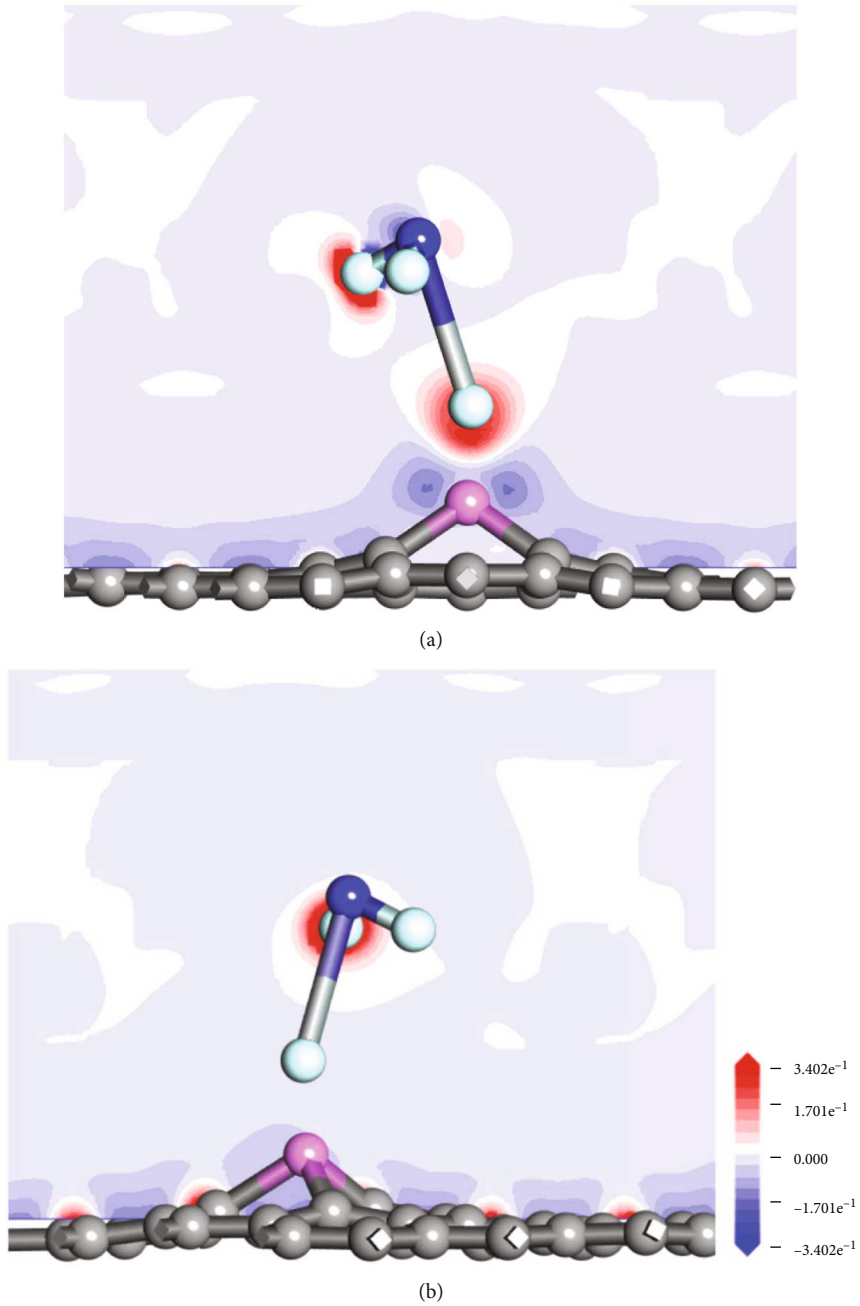

(a)

(b)

Figure 6: The charge difference density of NF_3 adsorbed on Al-Graphene ((a) F1 and F2 atom section; (b) F3 atom section).

difference in NF_3 electron density adsorbed on aluminum-doped graphene, it is obvious that the interaction between NF_3 and aluminum-doped graphene is very severe.

The band structure of aluminum-doped graphene without adsorbed gas exhibit in Figure 7(a). Figure 7(b) exhibit the band structure of NF_3 molecules adsorbed on aluminum-doped graphene surface. From above, it is known that the band structure of aluminum-doped graphene has an obvious band gap near the E_f, and a new energy level is introduced at the E_f. Moreover, a lot of new energy levels have been added in the valence band. It can be determined that the generation of the new energy level is due to the adsorption of gas on the surface.

3.3. The Adsorption Properties of N_2O on Aluminum-Doped Graphene. Gas molecules approach the aluminum-doped graphene surface with different atoms for the adsorption of N_2O. 3 characteristic adsorption structures are acquired following geometric optimization, according to Figure 8, the parameters of the above configurations are exhibited in Table 3. Figures 8(a) and 8(b) exhibits top and side view for M1 configuration. N_2O is close to the doped surface with an N1 atom, and the d_{ads} is 2.035 Å. The N1-N2 bond length of N_2O adsorbed on the surface reaches 1.142 Å, with the 1.180 Å N2-O bond length. The bond angle does not change, which is not different from the free N_2O molecule. Therefore, the N_2O structure shows low alterations in adsorption.

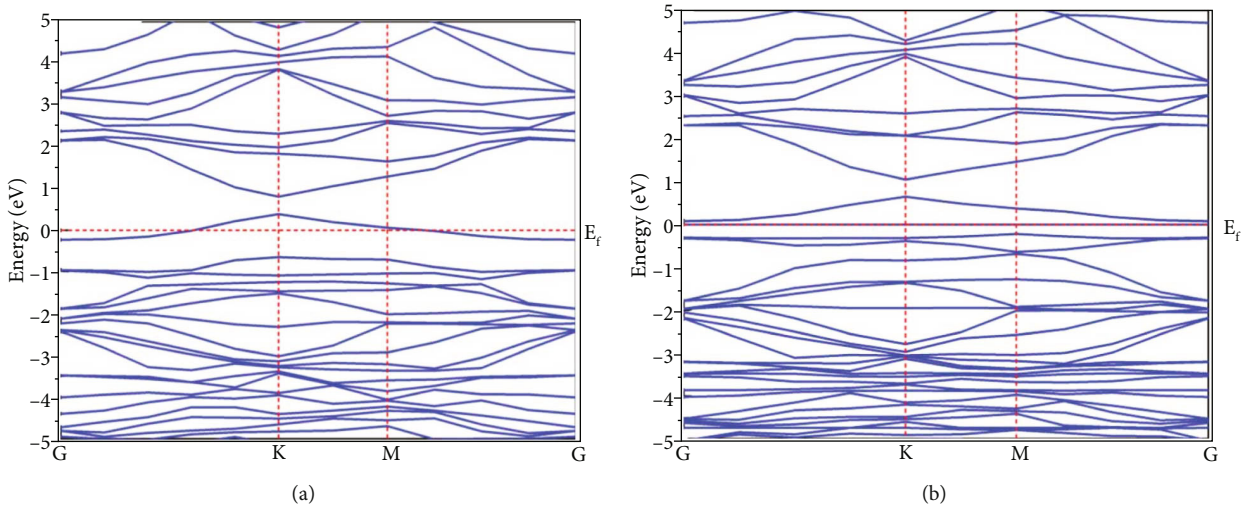

Figure 7: The band structure of Al-Graphene and NF_3 adsorption on Al-Graphene ((a) Al-Graphene; (b) NF_3-F-Al-Graphene).

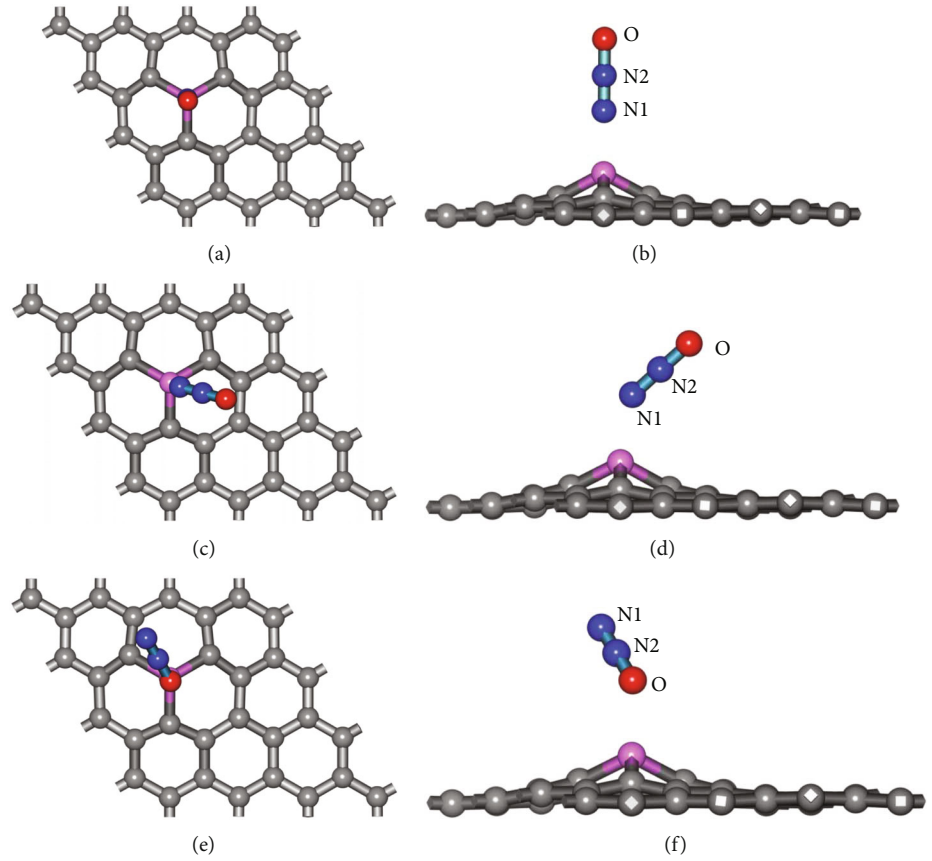

Figure 8: Adsorption configuration of N_2O adsorbed on Al-Graphene ((a) M1 top view; (b) M1 side view; (c) M2 top view; (d) M2 side view; (e) M3 top view; (f) M3 side view).

Table 3: The E_{ad}, Q_t, and structural parameters of the N_2O-adsorbed Al-Graphene.

Configuration	E_{ad}(eV)	Q_t(e)	d_{ads}(Å)	d_{N1-N2}(Å)	d_{N2-O}(Å)
M1	-1.376	0.238	2.035	1.143	1.180
M2	-1.407	0.212	2.080	1.148	1.180
M3	-1.240	0.204	2.157	1.214	1.133

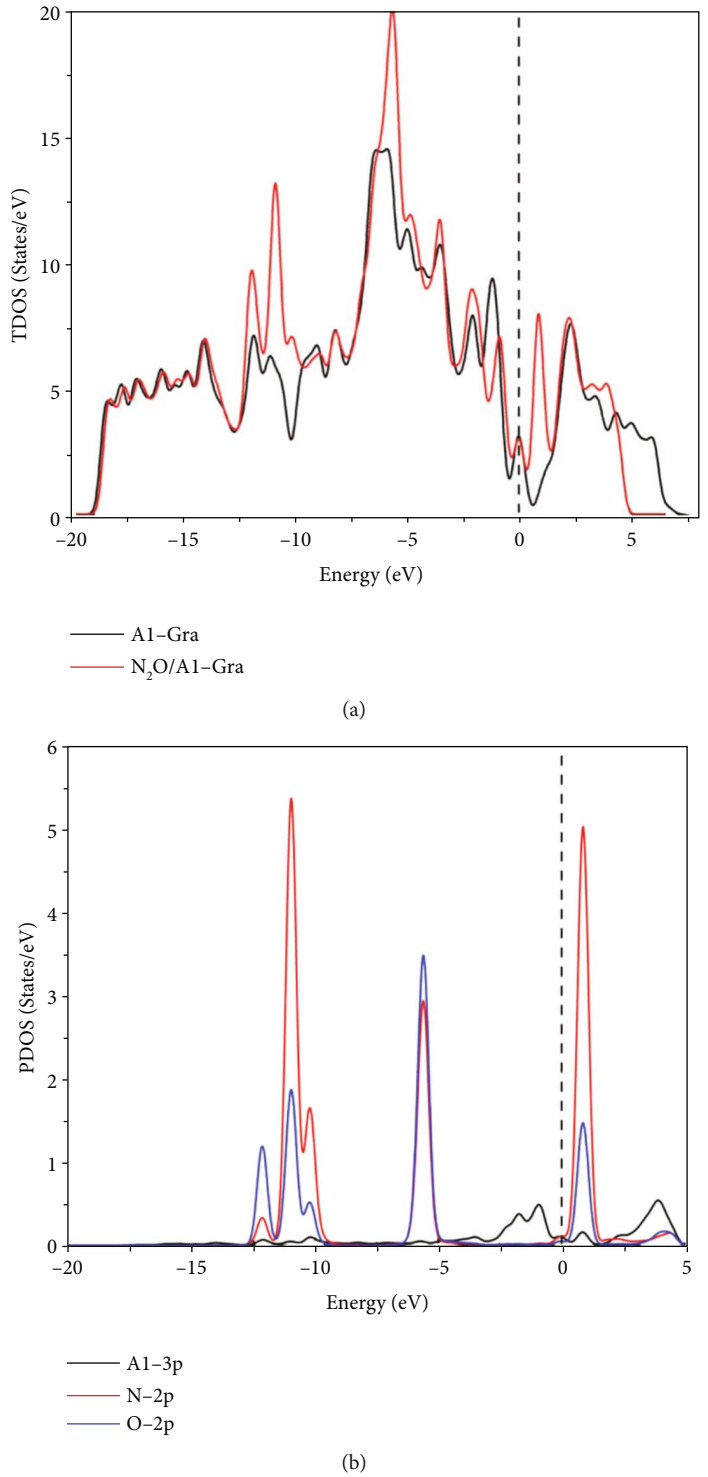

Figure 9: TDOS before and after N_2O adsorption and PDOS of the main interacting atoms ((a) TDOS; (b) PDOS).

In M1 configuration, adsorption energy is -1.376 eV, with the transfer of 0.238 e onto aluminum-doped graphene surface from the gas molecule, indicating the strong interaction between N_2O and aluminum-doped graphene surface.

Figures 8(c) and 8(d) exhibits side and top view for M2 configuration. N_2O is close to the doped surface with an N2 atom, and the d_{ads} is 2.080 Å. Based on structural parameters observed in Table 3, the N_2O structure has low alterations before and after adsorption. M2 configuration has adsorption energy of -1.407 eV, which indicates that the M2 configuration is more stable than M1. In addition, the transfer of 0.212e onto aluminum doped graphene surface

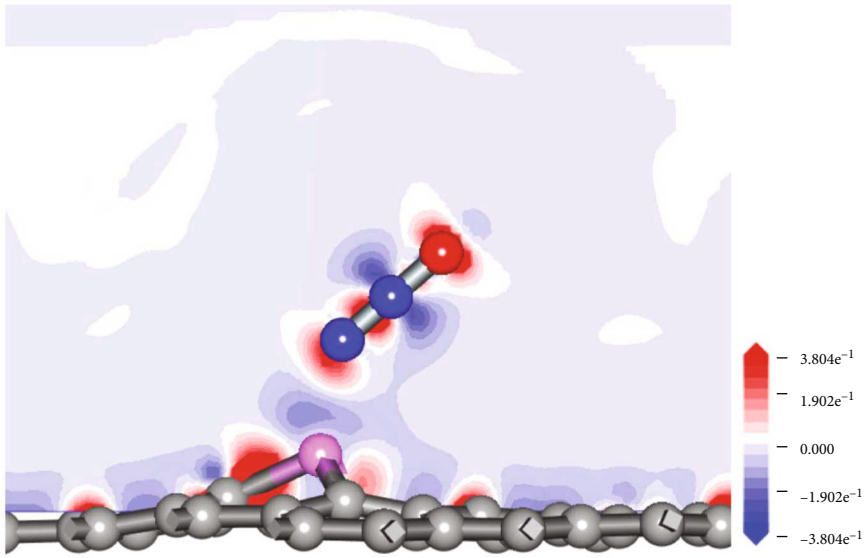

Figure 10: The charge difference density of N_2O adsorbed on Al-Graphene.

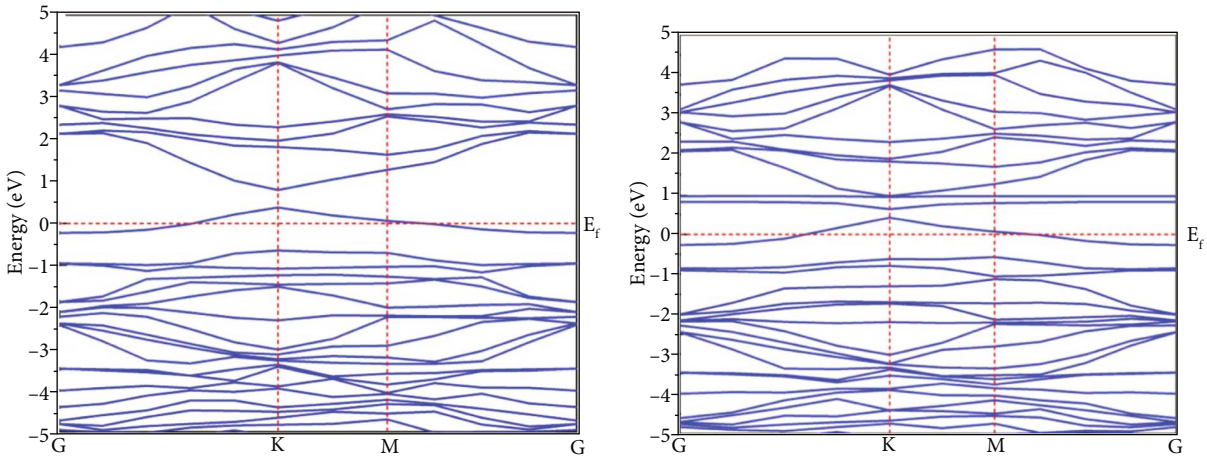

Figure 11: The band structure of Al-Graphene and N_2O adsorption on Al-Graphene ((a) Al-Graphene; (b) N_2O-N-Al-Graphene).

from gas molecules is detected in the M2 configuration, with the charges transferred from N1, N2, and O atom being 0.247 e, -0.004 e, and 0.031 e, respectively.

The side and top views for the M3 configuration are displayed in Figures 8(e) and 8(f). N_2O is close to the doped surface with the O atom, and the d_{ads} is 2.157 Å. The N1-N2 bond length of N_2O adsorbed onto aluminum-doped graphene surface reaches 1.214 Å, which is slightly longer than the N1-N2 bond (1.141 Å) of free N_2O molecules. The charge transfer in the M3 configuration is 0.204 e, which significantly increases relative to M1/M2 configuration. However, according to parameters observed in Table 3, the bond angle and bond length changed a little after adsorption, and the adsorption energy was -1.240 eV, which was slightly decreased when compared with the M2 configurations. In conclusion, this was based on great adsorption energy between N_2O and M2 configurations, and therefore, the M2 system may exhibit the highest stability. For better

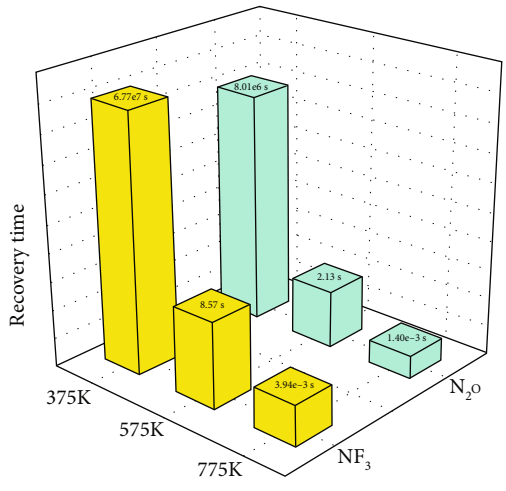

Figure 12: Desorption time at different temperatures.

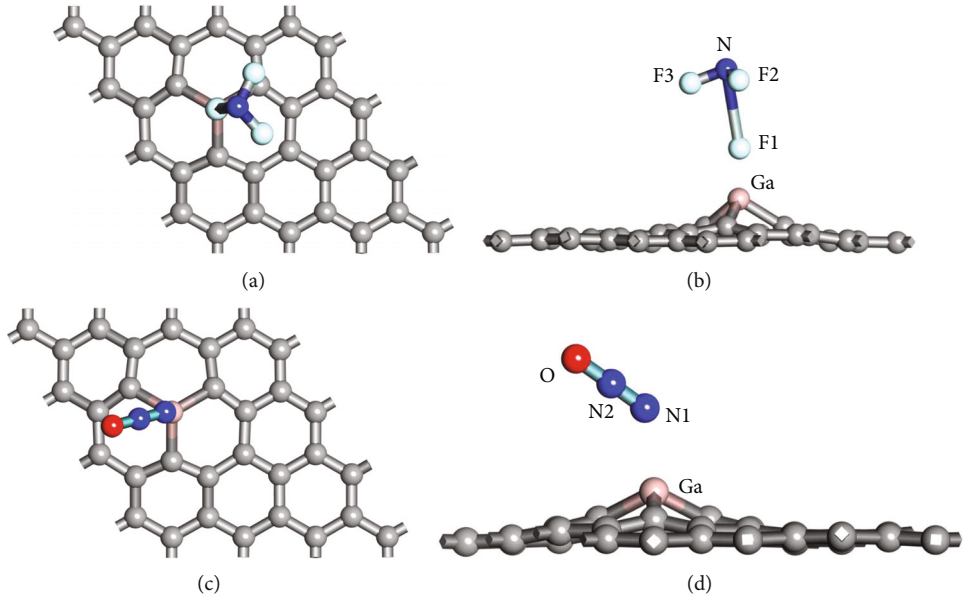

Figure 13: The adsorption configuration of NF_3 and N_2O adsorbed on Ga-Graphene ((a) X1 top view; (b) X1 side view; (c) X2 top view; (d) X2 side view).

verification, this work also analyzed the difference in electron density and DOS.

TDOS for M2 configuration is exhibited in Figure 9(a). When N_2O molecules are adsorbed onto an aluminum-doped graphene surface, there are obvious changes around -12.07 eV, -11.01 eV, -5.71 eV, and 0.89 eV. Due to the outermost electrons of atoms contributing the most to adsorption, this work only analyzes PDOS for Al-3p, N-2p, and O-2p. From PDOS observed in Figure 9(b), N-2p together with O-2p orbital peaks coincide around -12.15 eV, -10.97 eV, -10.25 eV, -5.62 eV, and 0.86 eV. According to PDOS, potent chemisorption of N_2O with aluminum-doped graphene was seen. At the same time, considering that the N-2p orbital contributes the most to the adsorption process, the N_2O adsorption structure shows extremely high stability within the M2 configuration.

The difference in electron density of M2 configuration is exhibited in Figure 10. Red and blue areas stand for elevated and declined electron densities, respectively. O and N1 receive charge in the adsorption process, and the charge close to the N2 atom declines. There is also an increase in electron density on the aluminum-doped graphene surface. According to the distribution on electron density, N_2O gets electrons.

The band structure of aluminum-doped graphene without adsorbed gas exhibit in Figure 11(a). Figure 11(b) shows the band structure of N_2O molecules adsorbed on aluminum-doped graphene surface. It can be seen that after adsorbing N_2O, the energy gap of aluminum doped graphene decreases, the conduction band near the Fermi level becomes more smooth, and introduced new energy levels. Accordingly, the density of states near the E_f increases greatly.

3.4. Prediction of Desorption of Aluminum-Doped Graphene. The decomposed components of SF_6/N_2 mixed gas can be desorbed from the sensing material surface under heating conditions. The E_{ad} and d_{ads} distance of NF_3 and N_2O on aluminum-doped graphene surface are exhibited in Tables 2 and 3, 375 K, 575 K, and 757 K are the temperature gradient of the desorption time of the sensing material. The desorption time is related to the adsorption energy and temperature, as shown in [32, 33]:

Table 4: The E_{ad}, Q_t, and structural parameters of the NF_3 and N_2O adsorbed on Ga-Graphene.

Configuration	E_{ad}(eV)	Q_t(e)	d_{ads}(Å)
X1	-1.356	0.287	1.801
X2	-1.280	0.227	2.285

$$\varepsilon = A^{-1} \exp\left(-E_{ad}/RT\right). \quad (3)$$

In which, A is the trial frequency of the system, generally $10^{12}\ s^{-1}$ [34], E_{ad} is the adsorption energy of NF_3 and N_2O on aluminum-doped graphene surface, R: a constant, eV/K, T is the temperature (unit: K).

The desorption time of NF_3 and N_2O gas molecules at 375 K, 575 K, and 775 K is shown in Figure 12. The optimal desorption time of NF_3 molecule at 775 K is 3.94×10^{-3} s, and the desorption time of the whole system increases with the decrease of temperature, and the maximum recovery time is 6.77×10^7 s. The desorption time of N_2O molecule in the system is shorter than that of NF_3 molecule. At 375 K and 775 K, the recovery time is 8.01×10^6 s and 1.40×10^{-3} s, respectively.

3.5. Adsorption of NF_3 and N_2O Gases on Gallium-Doped Graphene. Since the number of outermost electrons of Ga atom is the same as that of Al atom, the doping of Ga atom is also considered. Its adsorption mode is the same as that of Al doped graphene, so only consider that NF_3 molecules are close to Ga-doped graphene as F atoms, and N_2O molecules

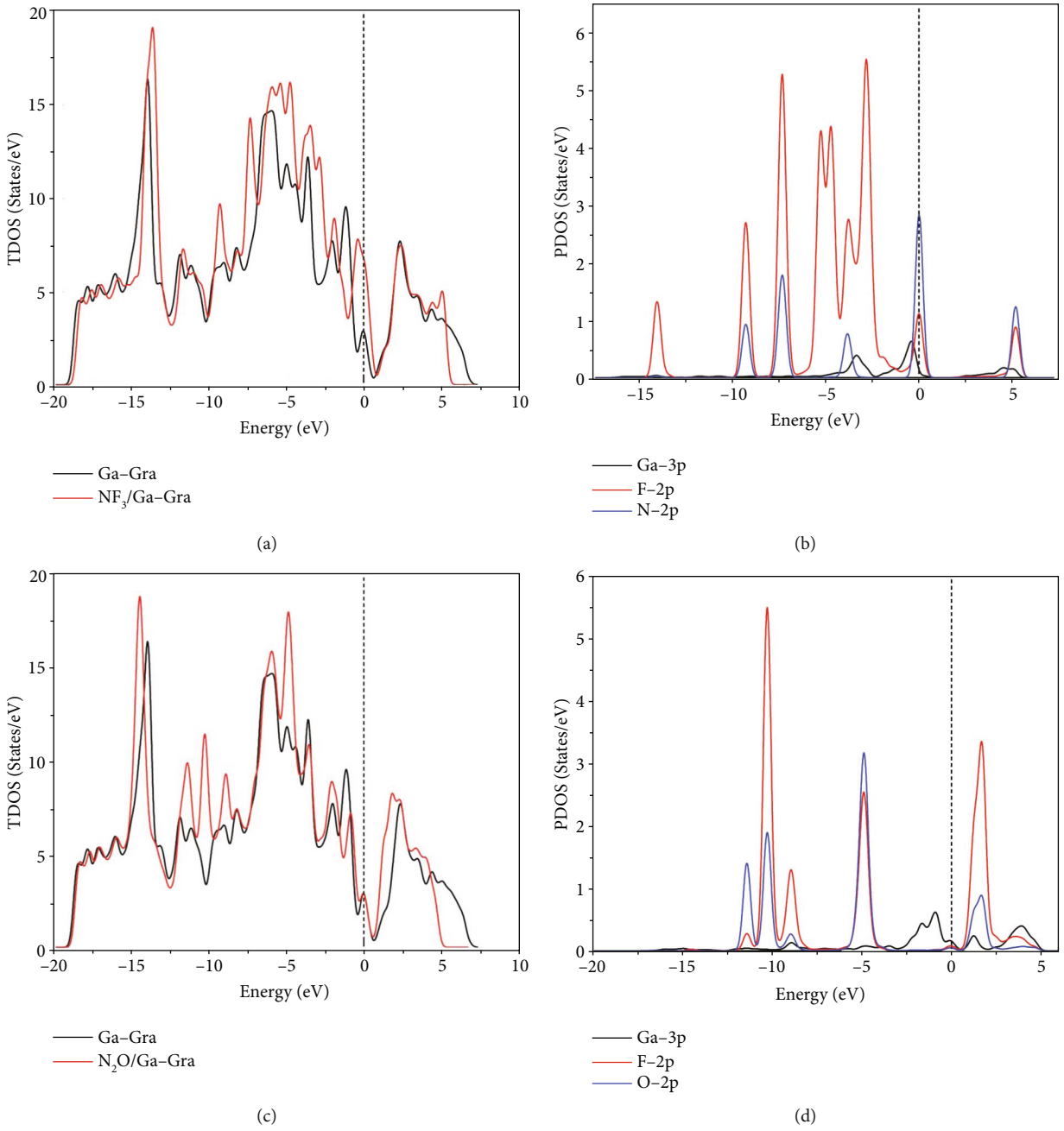

FIGURE 14: The density of states configuration of NF_3 and N_2O adsorbed on Ga-Graphene ((a) NF_3-TDOS; (b) NF_3-PDOS; (c) N_2O-TDOS; (d) N_2O-PDOS).

are close to Ga-doped graphene as N atoms. As shown in Figures 13(a) and 13(b), NF_3 molecules are adsorbed on Ga-doped graphene surface, the d_{ads} is 1.801 Å, and the electron transformation is 0.287 e. As shown in Figures 13(c) and 13(d), N_2O is adsorbed on Ga-doped graphene surface, the d_{ads} is 2.285 Å, and the electron transformation is 0.227 e. It can be seen from Table 4 that the adsorption energy of both gases is less than that on Al-doped graphene surface. The adsorption parameters show that there is a good reaction between NF_3 and N_2O molecules on Ga-doped graphene surface.

As shown in Figures 14(a)–14(d), it is the TDOS and PDOS of NF_3 and N_2O on Ga-doped graphene surface. For NF_3 molecule, a new peak appears at the E_f of PDOS, which is contributed by NF_3 molecule, where the 2p orbital of N atom, the 2p orbital of F atom, and the 3p orbital of Ga atom are coupled. For N_2O molecule, it can be seen from the PDOS diagram that there is no new peak at the E_f, and a fresh peak occur in the conduction band region, and it hybridizes with the 3p orbital of Ga atom, indicating that N_2O molecule has a strong interaction with Ga-doped graphene.

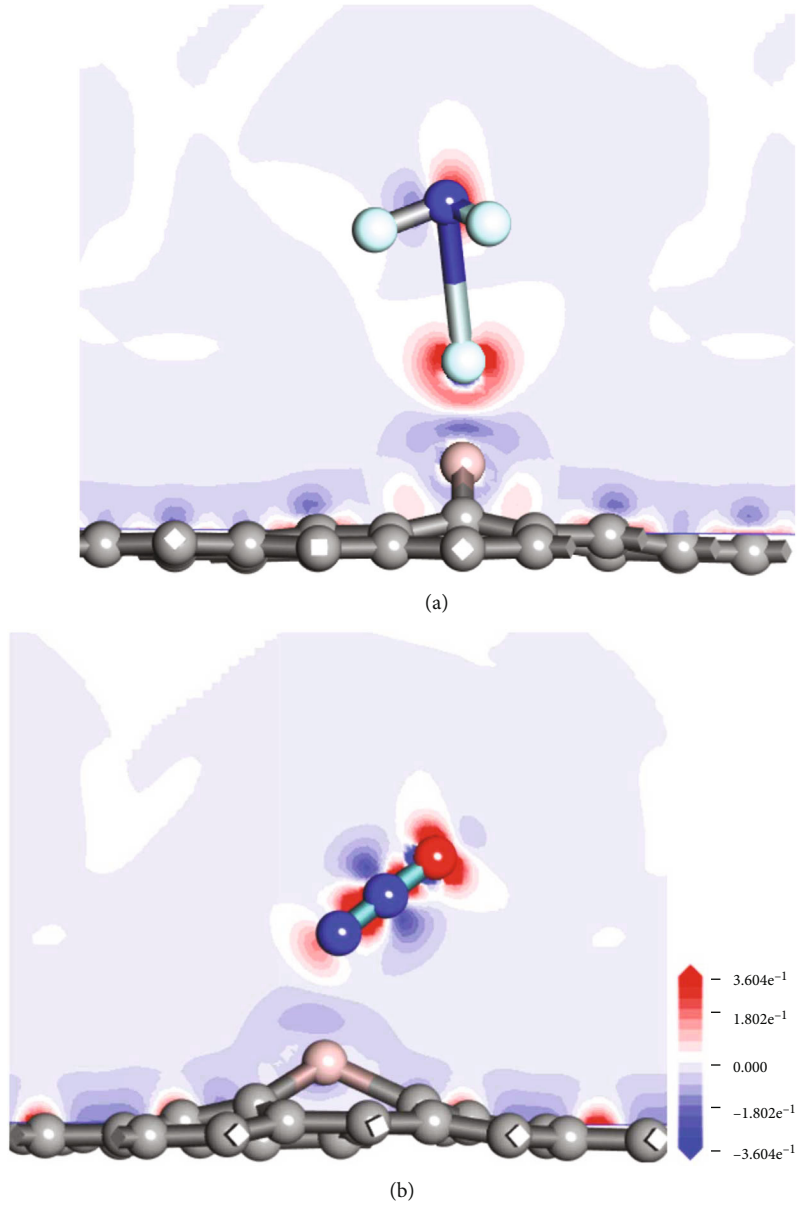

(a)

(b)

Figure 15: The charge difference density of NF_3 and N_2O adsorbed on Ga-Graphene ((a) the charge difference density of NF_3 adsorbed on Ga-Graphene; (b) the charge difference density of N_2O adsorbed on Ga-Graphene).

Figures 15(a) and 15(b) shows the charge difference density of NF_3 and N_2O on Ga-doped graphene, respectively. It can be seen that after the adsorption of NF_3 and N_2O, the color near F atom turns red, indicating that the charge increases, and the color near N atom turns blue, indicating that the charge decreases. The charge near N1 atom and O atom in N_2O molecule increases, and the electron concentration near N2 atom and graphene surface decreases, indicating that the gas obtains charge.

4. Conclusions

The adsorption characteristics of NF_3 and N_2O molecules on Al- and Ga-doped graphene surfaces were studied in this paper, for the sake of finding the resistance chemical sensor material for GIS internal fault diagnosis. Among them, the most likely adsorption mode of NF_3 molecule is that F atom is close to Al-doped graphene. They have large charge transfer and E_{ad}, short d_{ads}, and strong interaction. The most likely adsorption mode of N_2O molecules on Al-doped graphene is M2 mode, which is close to the N atom. From the adsorption parameters obtained, it can be seen that there is also a very strong interaction between N_2O molecules and Al-doped graphene. As Ga atom and Al atom belongs to the same family of elements, the simulation of Ga atom is also carried out. The results show that the adsorption parameters of Ga-doped graphene and Al-doped graphene are similar, and Ga-doped graphene may also be a sensing material.

The present work sheds more light on the association of characteristic decomposition components of SF_6/N_2 gas

mixture and Al- and Ga-doped graphene, and provides the theoretical foundation to adsorb characteristic decomposition components in SF_6/N_2 gas mixture onto Al- and Ga-doped graphene.

Conflicts of Interest

The authors declare that they have no conflicts of interest.

Acknowledgments

The authors would like to acknowledge the support of Science and Technology Research Program of Chongqing Municipal Education Commission (Grant No. KJZD-K202001505, KJQN202001503) and the Graduate Science and Technology Innovation Project of Chongqing University of Science and Technology (Grant No. YKJCX2120404).

References

[1] R. Ullah, A. Rashid, A. Rashid, F. Khan, and A. Ali, "Dielectric characteristic of dichlorodifluoromethane (R12) gas and mixture with N2/air as an alternative to SF6 gas," *High Voltage*, vol. 2, no. 3, pp. 205–210, 2017.

[2] M. Rabie and C. M. Franck, "An assessment of eco-friendly gases for elec-trical insulation to replace the most potent industrial greenhouse gas SF6," *Environmental Science & Technology*, vol. 52, no. 2, pp. 369–380, 2018.

[3] L. Fan, *Decomposition Characteristics of SF_6 under PD & Recognition of PD Category and Calibration of Impact Factors*, Chongqing University, Chongqing, 2013.

[4] X. Dengming, "Development prospect of gas insulation based on environmental protection," *High Voltage Engineering*, vol. 42, no. 4, pp. 1035–1046, 2016.

[5] Z. Wenjun, Y. Zheng, and Y. Shuai, "Research progress and trend of SF_6 alternative with environment-friendly insulation gas," *High Voltage Apparatus*, vol. 52, no. 12, pp. 8–14, 2016.

[6] W. Bin, S. Lichun, S. Wenxia, and G. Leguan, "SF_6 gas insulation and its global green house effect," *High Voltage Apparatus*, vol. 36, no. 6, pp. 23–26, 2000.

[7] Z. Anchun, G. Liying, and J. Xiao, "Research and application of SF_6/N_2 mixed Gas Used in GIS Bus," *Power System Technology*, vol. 42, no. 10, pp. 3429–3435, 2018.

[8] J. Yansong, Z. Min, W. Chengyu, and G. Leguan, "Detection methods and experimental study on decomposition products of SF_6/N_2 mixed gas," *High Voltage Apparatus*, vol. 56, no. 12, pp. 97–102, 2020.

[9] B. Szczesniak, J. Choma, and M. Jaroniec, "Effect of graphene oxide on the adsorption properties of ordered mesoporous carbons toward H_2, C_6H_6, CH_4 and CO_2," *Microporous and Mesoporous Materials*, vol. 261, pp. 105–110, 2018.

[10] T. Zhang, H. Sun, F. Wang et al., "Reversible adsorption/desorption of the formaldehyde molecule on transition metal doped graphene by controlling the external electric field: first-principles study," *Applied Surface Science*, vol. 136, no. 12, p. 134, 2017.

[11] X. Chen, X. Lei, L.-L. Liu et al., "Adsorption of formaldehyde molecule on the pristine and transition metal doped graphene: first-principles study," *Applied Surface Science*, vol. 396, pp. 1020–1025, 2017.

[12] A. S. Rad, "Adsorption of C_2H_2 and C_2H_4 on Pt-decorated graphene nanostructure: Ab-initio study," *Synthetic Metals*, vol. 211, pp. 115–120, 2016.

[13] X. He, Y. Gui, K. Liu, and L. Xu, "Comparison of sensing and electronic properties of C_2H_2 on different transition metal oxide nanoparticles (Fe_2O_3, NiO, TiO_2) modified BNNT (10, 0)," *Applied Surface Science*, vol. 521, article 146463, 2020.

[14] C. Qinchuan, D. Ziqiang, Q. Chen, and J. Tang, "A DFT study of SO2and H_2S gas adsorption on au-doped single-walled carbon nanotubes," *Physics*, vol. 89, no. 6, article 065803, 2014.

[15] A. Syaahiran, C. M. Lim, M. Kooh, A. H. Mahadi, Y. F. Chou Chau, and R. Thotagamuge, "A theoretical insight of Cr dopant in tungsten oxide for gas sensor application," *Materials Today Communications*, vol. 28, no. 10, article 102508, 2021.

[16] M. A. Syaahiran, A. H. Mahadi, C. M. Lim et al., "Theoretical Study of CO Adsorption Interactions with Cr-Doped Tungsten Oxide/Graphene Composites for Gas Sensor Application," *ACS Omega*, vol. 7, no. 1, pp. 528–539, 2022.

[17] Y. Gui, X. Peng, K. Liu, and Z. Ding, "Adsorption of C_2H_2, CH_4 and CO on Mn - doped graphene: Atomic, e1ectronic, and gas-sensing properties," *Physica E. Low -Dimensiona 1 Systems & Nanostructures*, vol. 119, article 113959, 2020.

[18] J. Sun and P. Zhang, "Gas adsorption properties of graphene doped with Pt/Pd," *Journal of Hebei Normal University*, vol. 38, no. 5, 2014.

[19] S. Peng, M. Zhao, G. Cui, and X. Jiang, "A theoretical study on the cyclopropane adsorption onto the copper surfaces by density functional theory and quantum chemical molecular dynamics methods," *Journal of Molecular Catalysis A: Chemical*, vol. 220, no. 2, pp. 189–198, 2004.

[20] B. Delley, "$Dmol^3$ DFT studies: from molecules and molecular environments to surfaces and solids," *Computational Materials Science*, vol. 17, no. 2-4, pp. 122–126, 2000.

[21] C. Di Valentin, G. Pacchioni, A. Selloni, S. Livraghi, and E. Giamello, "Characterization of paramagnetic species in N-doped TiO_2 powders by EPR spectroscopy and DFT calculations," *The Journal of Physical Chemistry. B*, vol. 109, no. 23, pp. 11414–11419, 2005.

[22] J. P. Perdew, K. Burke, and M. Ernzerhof, "Generalized gradient approximation made simple," *Physical Review Letters*, vol. 77, no. 18, pp. 3865–3868, 1996.

[23] J. P. Perdew, J. A. Chevary, S. H. Vosko et al., "Atoms, molecules, solids, and surfaces: applications of the generalized gradient approximation for exchange and correlation," *Physical Review B: Condensed Matter*, vol. 46, no. 11, pp. 6671–6687, 1992.

[24] S. N. Maximof, M. Ernzehof, and G. E. Scuseria, "Current-dependent extension of the Perdew–Burke–Ernzerhof exchange-correlation functional," *The Journal of Chemical Physics*, vol. 120, no. 5, pp. 2105–2109, 2004.

[25] Y. Inada and H. Orita, "Efficiency of numerical basis sets for predicting the binding energies of hydrogen bonded complexes: evidence of small basis set superposition error compared to Gaussian basis sets," *Journal of Computational Chemistry*, vol. 29, pp. 225–232, 2008.

[26] N. A. Karim, S. K. Kamarudin, L. K. Shyuan, Z. Yaakob, W. R. W. Daud, and A. A. H. Khadum, "Novel cathode catalyst for DMFC: study of the density of states of oxygen adsorption using density functional theory," *International Journal of Hydrogen Energy*, vol. 39, no. 30, pp. 17295–17305, 2014.

[27] Z. Bo, X. Guo, X. Wei, H. Yang, J. Yan, and K. Cen, "Density functional theory calculations of NO_2 and H_2S adsorption on the group 10 transition metal (Ni, Pd and Pt) decorated graphene," *Physica E Low Dimensional Systems & Nanostructures*, vol. 109, pp. 156–163, 2019.

[28] W. Yao, G. Yingang, J. Chang et al., "Adsorption of SF_6 decomposition components on Pt_3-TiO_2(1 0 1) surface: A DFT study," *Applied Surface Science*, vol. 459, pp. 242–248, 2018.

[29] C. Hao, Z. Xiaoxing, Z. Jun, and J. Tang, "Adsorption behaviour of SF6decomposed species onto Pd_4-decorated single-walled CNT: a DFT study," *Molecular Physics*, vol. 116, no. 13, pp. 1749–1755, 2018.

[30] H. Wei, Y. Gui, J. Kang, W. Wang, and C. Tang, "A DFT Study on the Adsorption of H_2S and SO_2 on Ni Doped MoS_2 Monolayer," *Nanomaterials*, vol. 8, no. 9, p. 646, 2018.

[31] Z. Wei, T. Chao, X. Jufang, and Y. Gui, "Micro-scale effects of nano-SiO_2 modification with silane coupling agents on the cellulose/nano-SiO_2 interface," *Nanotechnology*, vol. 30, no. 44, pp. 1361–6528, 2019.

[32] K. Patel, B. Roondhe, S. D. Dabhi, and P. K. Jha, "A new flatland buddy as toxic gas scavenger: a first principles study," *Hazardous Mater*, vol. 351, pp. 337–345, 2018.

[33] Y. H. Zhang, Y. B. Chen, K. G. Zhou et al., "Improving gas sensing properties of graphene by introducing dopants and defects: a first-principles study," *Nanotechnology*, vol. 20, no. 18, article 185504, 2009.

[34] S. Peng, K. Cho, P. Qi, and H. Dai, "Ab initio study of CNT NO_2 gas sensor," *Chemical Physics Letters*, vol. 387, no. 4-6, pp. 271–276, 2004.